Elamawi et al. Egyptian Journal of Biological Pest Control (2018) 28:28
DOI 10.1186/s41938-018-0028-1

Egyptian Journal of Biological Pest Control

RESEARCH Open Access

Biosynthesis and characterization of silver nanoparticles using *Trichoderma longibrachiatum* and their effect on phytopathogenic fungi

Rabab M. Elamawi[1*], Raida E. Al-Harbi[2] and Awatif A. Hendi[3]

Abstract

An efficient biosynthesis process for the rapid production of nanoparticles would enable the development of a "microbial nanotechnology" for mass-scale production. In the present research, biological silver nanoparticle was synthesized extracellularly by using the fungus, *Trichoderma longibrachiatum*, where the cell filtrate of the fungus was used as a reducing and stabilizing agent in the process of nanoparticle synthesis. Different physical parameters such as fungal biomass concentration (1, 5, 10, 15, and 20 g), temperature (25, 28, and 33 °C), incubation time (0–120 h) , and agitation (shaken or not shaken) were investigated, in order to determine the optimal conditions for nanoparticle biosynthesis. The stability and antifungal properties of the synthesized silver nanoparticles (AgNPs) were also determined. Data revealed that a combination of 10 g fungal biomass, a reaction temperature of 28 °C, a 72-h incubation time, and without shaking were the optimum conditions for the synthesis of the silver nanoparticles. Visual observation of brown color is an indication of silver nanoparticle production. UV–vis spectroscopy showed maximum absorption at 385 nm with the optimum conditions. Transmission electron microscopy (TEM) revealed the formation of monodispersed spherical shape with a mean diameter of 10 nm. Fourier transformation infrared (FTIR) showed bands at1634.92 and 3269. 31 cm^{-1}. Dynamic light scattering (DLS) supported that the *Z*-average size was 24.43 and 0.420 PdI value. Zeta potential showed − 19.7 mV with a single peak. The AgNPs synthesized through this biosystem approach were relatively stable up to 2 months after synthesis. The use of AgNPs as antifungal led to significant reductions in the number of forming colonies for many plant pathogenic fungi, with efficiencies reaching up to 90% against *Fusarium verticillioides*, *Fusarium moniliforme*, *Penicillium brevicompactum*, *Helminthosporium oryzae*, and *Pyricularia grisea*. However, further research should be carried out in order to determine the toxic effect of AgNPs before mass production and use of agricultural applications.

Keywords: *Trichoderma longibrachiatum*, Silver nanoparticles, UV–vis spectroscopy, TEM, FTIR, DLS, Zeta potential, Antifungal activity

Background

Silver nanoparticles are widely used in many applications in various fields such as bio-labeling, sensors, antimicrobial agents, filters, microelectronics, and catalysis. This is because of their specific physico-chemical and biological properties (Pal et al. 2007; Ingle et al. 2008; Kim et al. 2008; Rai et al. 2009). Silver nanoparticles (AgNPs) have inhibitory effects on the growth of bacteria, virus, and other eukaryotic microorganisms (Jeong et al. 2005). In addition to their distinctive properties, their production cost is relatively low (Capek 2004). Physical and chemical methods have been utilized for the synthesis of nanoparticles (Mandal et al. 2005; Solanki and Murthy 2010; Huang et al. 2011). Basically, the physical methods have affected low yields, while the chemical ones caused harmful effects on the environment due to use of toxic solvents and the regeneration of hazardous by-products (Wang et al. 2007). Biosynthetic methods have been investigated as an

* Correspondence: rabab.elamawi@yahoo.com
[1]Rice Pathology Department, Plant Pathology Research Institute, Agricultural Research Center, PO Box 33717, Sakha, Kafr Elshiekh, Egypt
Full list of author information is available at the end of the article

alternative to chemical and physical methods. Microorganisms have been explored as potential bio-factories for synthesis of metallic nanoparticles such as cadmium sulphide, gold, and silver (Sastry et al. 2003). Biosynthesized nanoparticles are eco-friendly, reliable, biocompatible, and low cost (Roy et al. 2013; Emeka et al. 2014).

Silver nanoparticles may be less toxic to humans and animals than synthetic fungicides. Moreover, the toxicity that nanoparticles may cause in algae, plants, and fungi may be coupled with some positive effects (Sondi and Salopek-Sondi 2004). Recent studies in mammals and human cells have demonstrated that AgNPs are cytotoxic to various types of cells (Vandebriel et al. 2014; AshaRani et al. 2009). Other studies have shown that AgNPs accumulate in various types of cells (blood, liver, lungs, kidneys, stomach, testes, and brain) but showed no significant genotoxicity function (Kim et al. 2008). AgNPs effectively inhibit microorganisms without causing significant cytotoxicity also; AgNPs are nontoxic in mice and guinea pigs when administered by oral, ocular, and dermal routes. These conflicting results reveal the difficulty of pinpointing the overall toxicity of AgNPs to humans because the tremendous variation in particle size, particle aggregation, and concentration or coating thickness (in implants) of AgNPs has different profiles of silver release and bioactivity. In short, much longer and detailed studies have to be carried out to seriously consider AgNPs' potential toxicity in humans (Sharma et al. 2009; Murphy et al. 2015).

Biologically synthesized AgNPs could have many applications (Schultz et al. 2000; Durán et al. 2005). Different genera of fungi have been reported to synthesize metal nanoparticles (Ahmad et al. 2003; Mukherjee et al. 2002; Sastry et al. 2003; Mandal et al. 2005).

The fungal genus *Trichoderma* (Ascomycetes, Hyprocreales) contains species that are of vast economic importance owing to their production of industrial enzymes and antibiotics (Sivasithamparam and Ghisalberti 1998) and their ability to act as biological control agents against plant pathogens. In the biosynthesis of metal nanoparticles by a fungus, its mycelium is exposed to the metal salt solution, which prompts the fungus to produce enzymes and metabolites for its own survival. In this process, the metal ions are reduced to the metallic solid nanoparticles through the catalytic effect of the extracellular enzyme and metabolites of the fungus (Das and Marsili 2010; Vahabi et al. 2011).

The objectives of the present work were to determine the optimal conditions for the synthesis of biogenic silver nanoparticles, using a filtrate of the fungus *T. longibrachiatum* and its characterization, and also the stability and antimicrobial activity of the synthesized AgNPs against phytopathogenic fungi.

Materials and methods

Isolation and identification of fungal isolates

Fungal isolates were collected from cucumber, tomato, and pepper plants from around Alryadah city, Saudi Arabia, during 2013 and purified, using hyphal tip standard techniques, and maintained on a potato dextrose agar (PDA) slant and stored at 4 °C until further use. Fungal isolates were identified as *T. longibrachiatum* (cucumber), *T. viride* (cucumber), *T. harzianum* (tomato), *F. verticillioides* (pepper), *Alternaria alternate* (tomato), and *Rhizopus stolonifer* (pepper) based on the publication by Barnett and Hunter (1995). Further identification was done by Nano Technology Center for Scientific Services in Egypt, using fingerprint biotechnology according to Harman et al. (2004) and Harman (2006). Three Trichoderma species viz. *T. longibrachiatum*, *T. viride*, and *T. harzianum* were screened for their ability to synthesize silver nanoparticles. The isolates were cultured in PDA and incubated at 25 °C for 5 days and used for extracellular syntheses of silver nanoparticles. The fungal isolates; *F. moniliforme*, *A. flavus*, *P. grisea*, and *H. oryzae* were obtained from Rice Pathology Department, Sakha, Kafr Elshiekh.

Fungal biomass preparation for AgNP biosynthesis

Two disks (5 mm in diameter) of each fungus were inoculated onto 100 ml of liquid medium containing (g/l) KH_2PO_4 7.0, K_2HPO_4 2.0, $MgSO_47H_2O$ 0.1, $(NH_4)_2SO4$ 1.0, yeast extract 0.6, and glucose 10. The flasks were incubated in a shaker at 150 rpm at 25–28 °C. After 120 h of growth, the pale white fungal mycelium took the shape of a circular mat (Fig. 1a). Then, the biomass was harvested by sieving through a Whatman filter paper no.1, followed by extensive washing with Milli-Q deionized water to remove any adhering medium parts from the biomass.

Optimization conditions for biosynthesis of silver nanoparticles

The effect of fungal biomass (5, 1, 10, 15, and 20 g), temperature (23, 28, and 33 °C), and agitation on constant shaking at150 rpm or without agitation were studied by varying one parameter at a time, keeping the other experimental conditions the same.

Biosynthesis of silver nanoparticles

Experiments were conducted with the fungal biomass and with a liquid medium in parallel. The fungal biomass was brought into contact with 100 ml Milli-Q deionized water for 48 h at 28 °C at150 rpm. After filtration by Whatman filter paper no.1, 50 ml of 1 mM $AgNO_3$ solution was mixed with 50 ml of cell filtrate in a 250 ml Erlenmeyer flask, kept on a shaker at 150 rpm

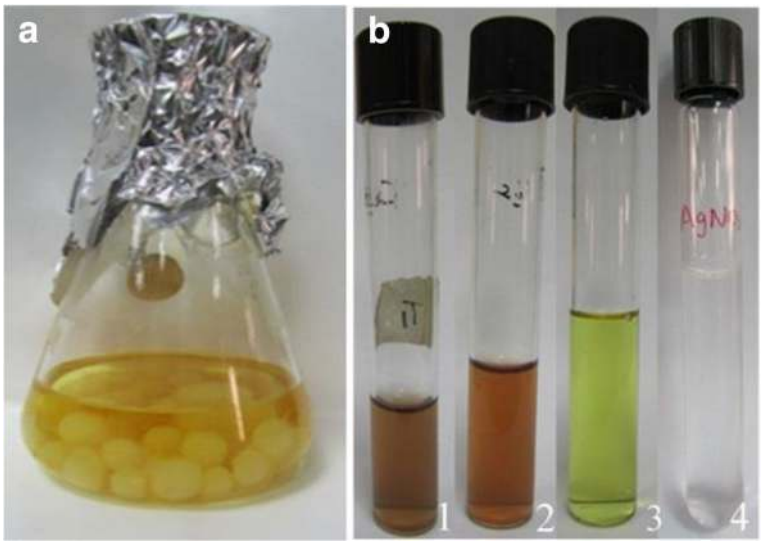

Fig. 1 Culture matt of fungus *Trichoderma longibrachiatum* in liquid media (**a**). **b** Biosynthesis of silver nanoparticle color change reaction after exposure to $AgNO_3$ solution for 96 h: (1) *T. viride*, (2) *T. harzianum*, (3) *T. longibrachiatum*, (4) $AgNO_3$ 1 mM solution

or without shaking at 23, 28, and 33 °C in the dark. The positive control is the only fungal biomass filtrate without the silver nitrate solution, and the negative control is the silver nitrate solution without cell-free filtrate. The reduction of metal ions was routinely monitored by visual inspection of the solution (color change from yellow to brown) and by measuring the ultraviolet-visible spectrophotometer of the solution by periodic sampling of aliquots (1 ml) of the aqueous component. The formed silver nanoparticles were subjected to different instrumental analytical techniques for characterization.

Characterization of silver nanoparticles

Ultraviolet-visible spectrophotometer analysis

The formation of the reduced silver nanoparticles in colloidal solution was monitored by using a UV–vis spectrophotometer (Lambda 25, PerkinElmer, precisely, UK). The absorption spectra of the supernatants were taken between 300 and 700 nm, using a UV–vis spectrophotometer. The deionized water was used as the blank.

Fourier transform infrared (FTIR) spectroscopy

The FTIR spectrum of biosynthesized silver product was recorded on a FTIR instrument mode Nicolet 6700 spectrometer at a resolution of 4 cm^{-1} attachment. All measurements were carried out in the range of 400–4000 cm^{-1} at a resolution of 4 cm^{-1}.

Transmission electron microscopy (TEM)

TEM was performed on JEOL, Japan (JEM-1010) instrument, within accelerating voltage of 80 kV after drying of a drop of aqueous AgNPs on the carbon coated copper. TEM grid samples were dried and kept under vacuum in desiccators before loading on a specimen holder. The particle size distribution of AgNPs was evaluated using ImageJ 1.45 s software1493.

Dynamic light scattering

Zetasizer Nano ZS, Malvern Instruments Ltd., UK, was used to determine the size distribution of particles by measuring dynamic fluctuations of light scattering intensity caused by the Brownian motion of the particles. The measurement gave the average hydrodynamic diameter of the particles, the peak values in the hydrodynamic diameter distribution, and the polydispersity index (PdI) that described the width of particle size distribution. The PdI scale ranges from 0 to 1 (with 0 being monodisperse and 1 being polydisperse). All measurements were carried out in triplicate with a temperature equilibration time of 1 min at 25 °C. The data processing mode was set to high multi-modal resolution. The suspension of the synthesized silver nanoparticles was diluted (20, 40, 60, 80, and 100%), and the diluted sample was allowed to filter through a 0.22-μm syringe driven filter unit or without filtration.

Antifungal activity for AgNPs synthesized in in vitro assays

The antifungal activity of nanoparticles was examined on the basis of colony formation technique by in vitro Petri dish (Elamawi and El-Shafey 2013). The antifungal activity of the synthesized AgNPs was examined against the pathogenic fungi: *A. alternate*, *F. oxysporum*, *F. verticillioides*, *F. moniliforme*, *Aspergillus flavus*, *A. heteromorphus*, *P. glabrum*, *P. brevicompactum*, *P. grisea*, and *H. oryzae*. Fungal

spores at a concentration of 10^5 spores/ml were incubated at 0.5 mM AgNP solution, 1 mM $AgNO_3$ solution, and sterile, distilled water as a control at 28 °C for 24 h in a shaker (120 rpm). A 25-μl aliquot of the spore suspension was spread on PDA. Three PDA plates per combination were used as replicates. The number of formed colonies was counted after 24 and 48 h. The average numbers of colonies from silver-treated spore suspensions were compared to the number of colonies of $AgNO_3$ solution and with the control (water treatment).

Statistical analysis

The null hypothesis may be rejected, and there is a 95% confidence level that the parameters are not the same as were tested, using one-way analysis of variance (ANOVA), followed by LSD post hoc test, when significant differences were found ($P \leq 0.05$). Statistical significance of results obtained from treating fungi with both Ag-NPs and $AgNO_3$ were compared to control.

Results and discussion

Characterization of AgNPs

Three Trichoderma species viz. *T. longibrachiatum*, *T. viride*, and *T. harzianum* were used for biosynthesis of stable AgNPs. Filtrates of each fungal isolates were incubated with $AgNO_3$ and maintained with agitation under dark conditions at 28 °C. Color change from pale yellow to brown appeared after the incubation period of 72 h with the *T. harzianum* and *T. viride*, but there was no color change with *T. longibrachiatum* (Fig. 1b). The appearance of the brown color was an indication of the formation of AgNPs in the medium. The positive control (without the $AgNO_3$ solution, only fungal biomass) and the negative control (pure $AgNO_3$ solution without cell-free filtrate) did not show any change of color for the mixture reaction (Fig. 1b). The above conditions were recommended for the production of silver nanoparticles from *T. harzianum* and *T. viride*. However, it could not be recommended to produce silver nanoparticles from *T. longibrachiatum*. So, optimization of some factors affecting silver production from *T. longibrachiatum* is required.

UV–visible spectrum of the biosynthesis of silver nanoparticles using the fungi of *T. harzianum* and *T. viride* showed a peak at 420 and 420 nm corresponding to the plasmon absorbance of silver nanoparticles for the tested fungi *T. harzianum* and *T. viride*, respectively. Particle size analysis using TEM of AgNPsof *T. harzianum* and *T. viride* showed a formation of polydispersed AgNPs in a range of 30–50 nm with *T. harzianum* and 5–40 nm with *T. viridi*, as reported by Fayaz et al. (2010) and Singh and Balaji (2011).

Optimization conditions for biosynthesis of silver nanoparticles

Effect of quantity of fungal biomass and agitation

Five different quantities of fungal biomass of *T. longibrachiatum* (1, 5, 10, 15, and 20 g) were subjected to 1 mM $AgNO_3$ solution, incubated at 28 °C, with or without agitation. The mixture reaction showed a change in color from light yellow to dark brown after 72 h of incubation without shaking with the amounts of 5, 10, 15, and 20 g fungal biomass (Fig. 2).

The UV–visible absorption spectroscopy of *T. longibrachiatum* was measured by the fungal biomass 10, 15, and 20 g at different times (72, 96, and 120 h) of reaction time as presented in Fig. 3. It was observed that the formation of AgNPs increases with the increase of the quantity of fungal biomass. The time of reaction started at 72 h and maximized at 120 h without significant differences between quantities of fungal biomass. The range of absorbance was at 384 nm. This event clearly indicated that the reduction of the ions occurs extracellularly through reducing agents released into the solution by *T. longibrachiatum*. The control treatment without silver ions showed no change in color, when incubated under the same conditions. The color changes observed could be attributed to the surface plasmon resonance of deposited AgNPs. The increase in color intensity of culture filtrate was due to an increase in number of nanoparticles formed from the reduction of silver ions present in the aqueous solution. The amount of fungal biomass was a key parameter that affects the process of AgNP synthesis from *T. longibrachiatum*.

Effect of temperature

Three temperatures 23, 28, and 33 °C with five quantities of fungal biomass, without agitation, in the presence of 1 mM $AgNo_3$ were tested. The temperature of 28 °C was favorable for the production of AgNPs by *T. longibrachiatum* where color changed after 72 h of incubation with $AgNO_3$. The UV–visible absorption spectroscopy of the *T. longibrachiatum* incubated at 28 °C showed a maximum absorbance at 385 nm. Incubation at 23 and 33 °C showed no change in color when incubated under the same conditions. Reaction temperature had an important effecton enzyme activity. Fayaz et al. (2009) found that the size of biosynthesized silver nanoparticles by T. viride ranged from 10 to 40 nm at 27 °C. While, at a lower temperature (10 °C), the size of silver nanoparticles ranged from 80 to 100 nm. Thus, these findings are different from those which showed that an increase in reaction temperature resulted in a decrease in particle size, whereas a decrease

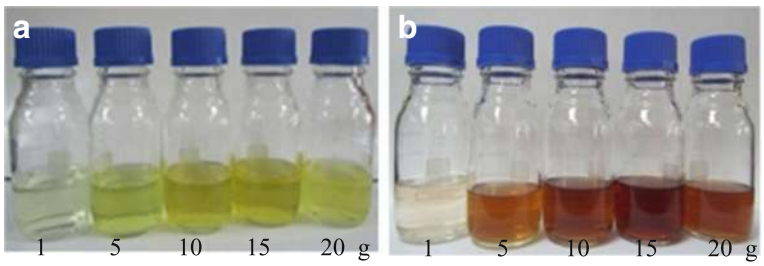

Fig. 2 Color change observed in cell-free fungal extract of *Trichoderma longibrachiatum* biomass after exposure to $AgNO_3$ ions at 28 °C with **a** agitation or **b** without agitation

in temperature resulted in an increase in particle size. This could be explained that 28 °C was favorable for biosynthesis of AgNPs by *T. longibrachiatum*, while 23 and 33 °C were unfavorable.

There is a relation between the particle size and the plasmon peak, as the particles became larger when the plasmon peak shifts to longer wavelengths. Values for Ag particle size and plasmon maxima that were reported with Solomon et al. (2007) indicated that UV spectra were in lower wavelengths (384–414), with 10- to 14-nm particle size. Nair and Pradeep (2003) revealed that UV spectra at 438 nm wavelength gave particle sizes of 60–80 nm. Obtained results indicated that lower wavelengths of UV spectra at 383 nm recorded particle sizes at 1–25 nm at 28 °C.

Effect of filtration

The effect of filtration on the AgNPs, produced from 10 or 15 g fungal biomass of *T. longibrachiatum*, using UV–vis spectrophotometer was illustrated in Fig. 4. The plasmon peak shifted to longer wavelengths (414 nm) with a fungal biomass of 10 g. No significant differences between non-filtered and filtered samples were observed with 15 g of fungal biomass, as the plasmon peak obtained by UV–vis spectrophotometer was 385 nm.

Parametric optimization studies revealed that fungal biomass of 10 or 15 g at 28 °C, without shaking or filtration, is favorable for the production of AgNPs by *T. longibrachiatum*. There was always a continuous interaction between the organisms and the environment they lived in.

FTIR spectroscopy analysis

The FTIR spectroscopy is very important to characterize the proteins binding with the AgNPs, and it is possible to quantify secondary structure in metal nanoparticle–protein interaction. FTIR spectroscopy was carried out on AgNPs synthesized with both 10 and 15 g fungal biomass formed after 96 h of incubation with $AgNO_3$. As shown in Fig. 5, FTIR spectrum revealed bands at 1634.92, 2156.94, and 3269.31 cm^{-1}. A band at 1634.92 cm^{-1} corresponded to the bending vibrations of the amide I and amide II bands of proteins (Gole et al. 2001), while their corresponding stretching vibrations of primary amines were observed at 3269.31 cm^{-1}. Similar FTIR spectrums were obtained with 10 or 15 g final biomass (Fig. 5). These observations indicated the presence and binding of proteins with AgNPs, which can lead to their possible stabilization and prevent agglomeration. FTIR results revealed that secondary structure of proteins had not been affected as a consequence of reaction with silver ions or binding with AgNPs (Jain et al. 2011). FTIR

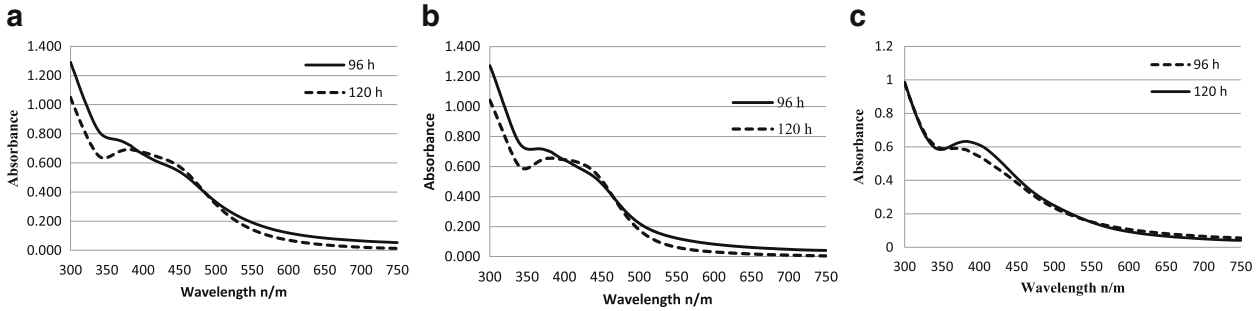

Fig. 3 a–**c** UV–visible absorption spectra of extracellularly synthesized AgNPs by *Trichoderma longibrachiatum* with fungal biomass 10g (**a**), 15 g (**b**) and 20g (**c**)

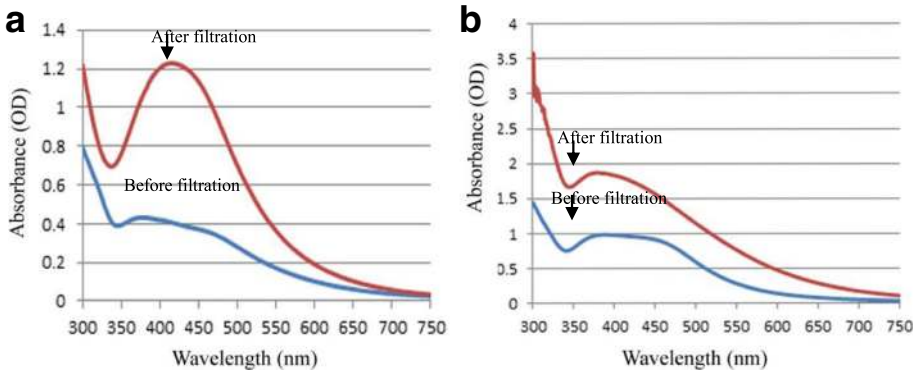

Fig. 4 UV–visible absorption spectrum of synthesized AgNPs by *Trichoderma longibrachiatum* for **a** 10 g biomass and **b** 15 g biomass, before and after filtration with filter size 0.22 μm

spectroscopic study confirmed that amino acid and peptides form a coat covering the silver nanoparticles. The presence of the signature peaks of amino acids supports the presence of proteins in cell-free filtrate as observed in UV–vis spectra. It is well known that nanoparticle–protein interactions can occur either through free amino groups or cysteine residues in proteins and via the electrostatic attraction of negatively charged carboxylate groups in enzyme proteins (Gole et al. 2001 and Mandal et al. 2005). The carbonyl groups of amino acid residues and peptides had strong ability to bind to silver (Balaji et al. 2009). The proteins present over the silver nanoparticle surface act as capping agents. These results agreed with the results obtained with *A. niger* (Jaidev and Narasimha 2010).

Transmission electron microscope

TEM images were taken for AgNPs of two fungal biomasses (10 and 15 g) before and after filtration. TEM micrograph images showed monodispersed roughly spherical shapes with variable sizes. The particle size distribution of the AgNPs (Fig. 6) showed an average count of 500 AgNPs with sizes ranging from 1 to 25 nm. AgNPs with sizes ≥ 5 nm accounted for 45.4% of particles, while those with sizes of ≥ 10 and ≥ 15 nm accounted 24.8 and 16%, respectively (Fig. 7). TEM micrographs taken before filtration showed aggregates and debris in both fungal biomass of 10 and 15 g. After the filtration, the TEM micrograph appeared clear and the AgNPs were spherical-shaped and monodispersed with sizes ranging from

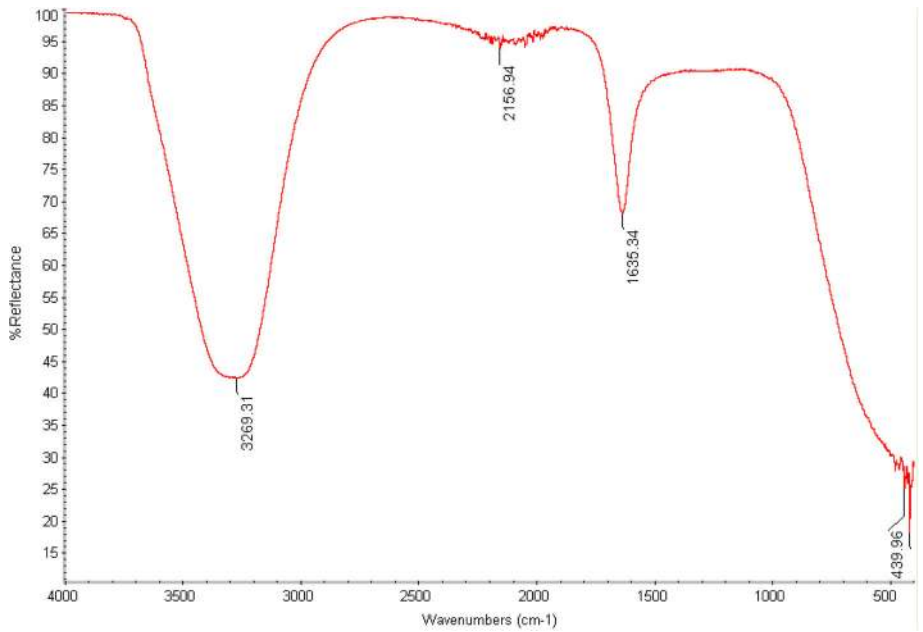

Fig. 5 Fourier transform infrared spectroscopy (FTIR) spectrum of AgNPs synthesized by reduction of Ag^{+} ions by *Trichoderma longibrachiatum*

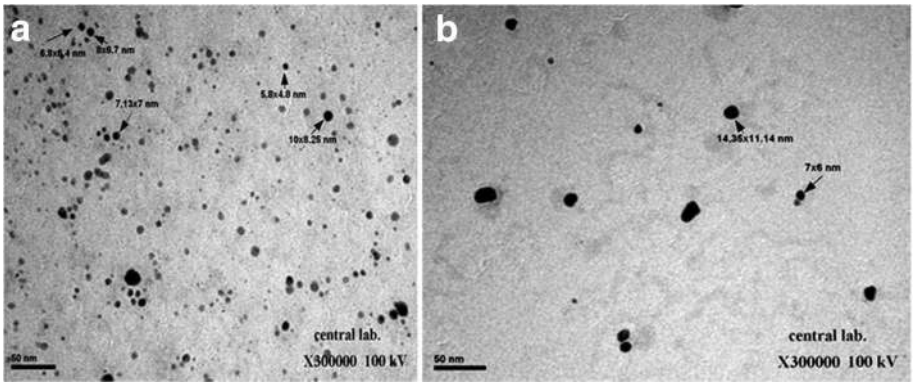

Fig. 6 TEM image of silver nanoparticles produced with *Trichoderma longibrachtium* after filtration of **a** 10 g fungal biomass and **b** 15 g fungal biomass

≤ 1 to 20 nm with 10 g fungal biomass. Fungal biomass of 15 g showed aggregation of silver nanoparticles. Monodispersed AgNPs with size ≥ 20 nm were observed after filtration. Two possible explanations of this observation could be proposed; first, the agglomeration might appear due to a possible accumulation of proteins and enzymes which were secreted during the biosynthesis, and second, the filtration might prevent the passing of different molecules of protein produced during the process of biosynthesis. The same type of the nanoparticles having variable shapes and sizes was observed in common biological systems in the range of 3–30 nm, when synthesized by *A. niger* (Jaidev and Narasimha 2010).

Particle size analysis of AgNPs by dynamic light scattering (DLS) system

The result of 10 g fungal biomass at 20% dilution without filtration, using DLS, showed good results. The data of DLS supported that the *Z*-average (r.nm) was 43.20. The average size of the synthesized AgNPs was 53.7 nm and 0.209 PdI value. The obtained single peak indicated that the quality of the synthesized silver nanoparticles was good (Fig. 8a). In the case of 15 g fungal biomass, the results were not good with all dilutions (unshown data). One peak was obtained with a wide base, indicating that variable sizes of AgNPs were found in the solution. For the filtered AgNP solution produced from 10 g fungal biomass, the data of DLS supported that the *Z*-average (r.nm) is with 24.43 nm and 0.420 PdI value (Fig. 8b). The average size of the synthesized AgNPs varied, and three peaks were observed at which with diameters of AgNPs were at 39.3, 4.4, and 1.5 nm.

The result of 15 g fungal biomass after filtration and using DLS showed good results. The *Z*-average size was 29.15 and 0.412 PdI value. Two peaks appeared showing AgNP diameters of 41.7 and 4.9 nm (Fig. 8c). Obtained results indicated that the value of the PdI, with 10 g fungal biomass, was 0.2 and 0.4 at dilution of 20 and 100%, before and after filtration, respectively. Moreover, AgNPs biosynthesized by *T. longibrachiatum* were nearly monodispersed with the various sizes ranging from 5 to 30 nm, in addition to the importance of filtration for removal of the aggregates. Obtained results from DLS

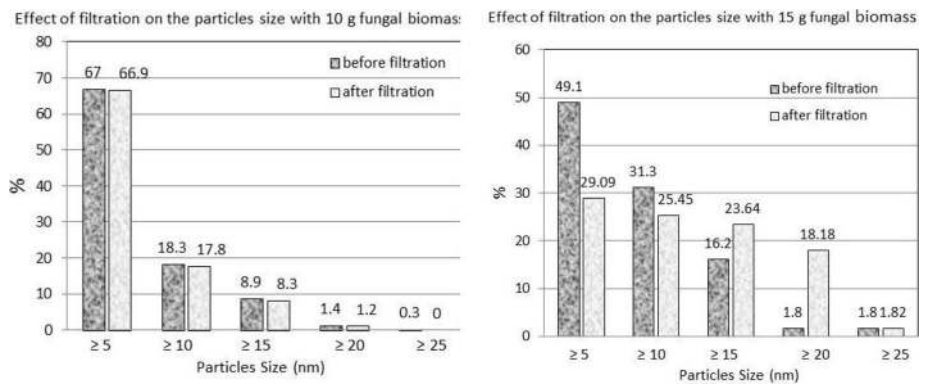

Fig. 7 Distribution of AgNP size from TEM analysis

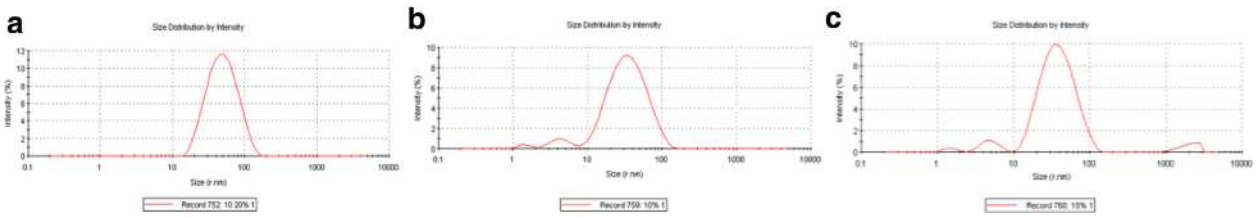

Fig. 8 Particle size distribution of AgNP solution synthesized by *Trichoderma longibrachiatum* for **a** 10 g fungal biomass at 20% dilution, **b** 10 g fungal biomass after filtration, and **c** 15 g fungal biomass after filtration

were in agreement with those obtained with TEM. The value of zeta potential of the silver nanoparticle solution produced from 10 g fungal biomass was − 19.7 mV, with a single peak signifying the presence of repulsion among the synthesized nanoparticles (Fig. 9a). Meanwhile, with the silver nanoparticle solution produced from 15 g fungal biomass, the value of zeta potential was − 4.33 mV (Fig. 9b). When all the particles in suspension have a large negative or positive zeta potential, they will tend to repel with each other and there will be no tendency of the particles to assemble together. However, if the particles have low zeta potential values, then there will be no force to prevent the particles from coming together and flocculating (Roy et al. 2013). The biosynthesized AgNPs were found to have negative zeta potential, which indicates the repulsion among the green synthesized silver nanoparticles and increases the stability of the formulation. It is evident that the AgNPs are polydispersed in nature, due to its high negative zeta potential; thus, the electrostatic repulsive force between them results in the prevention of agglomeration of the nanoparticles and is also very much helpful for long-term stability in the solution (Suresh et al. 2011 and Kotakadi et al. 2016).

Stabilization of AgNP synthesis by T. longibrachiatum against agglomeration

The stability of the synthesized particles was monitored for up to 60 days by using UV–vis spectral analysis, zeta potential. The UV–visible spectra of AgNPs showed an absorption peak at a wavelength of 414 nm. Moreover, the *Z*-average size of AgNPs was 90.27 nm

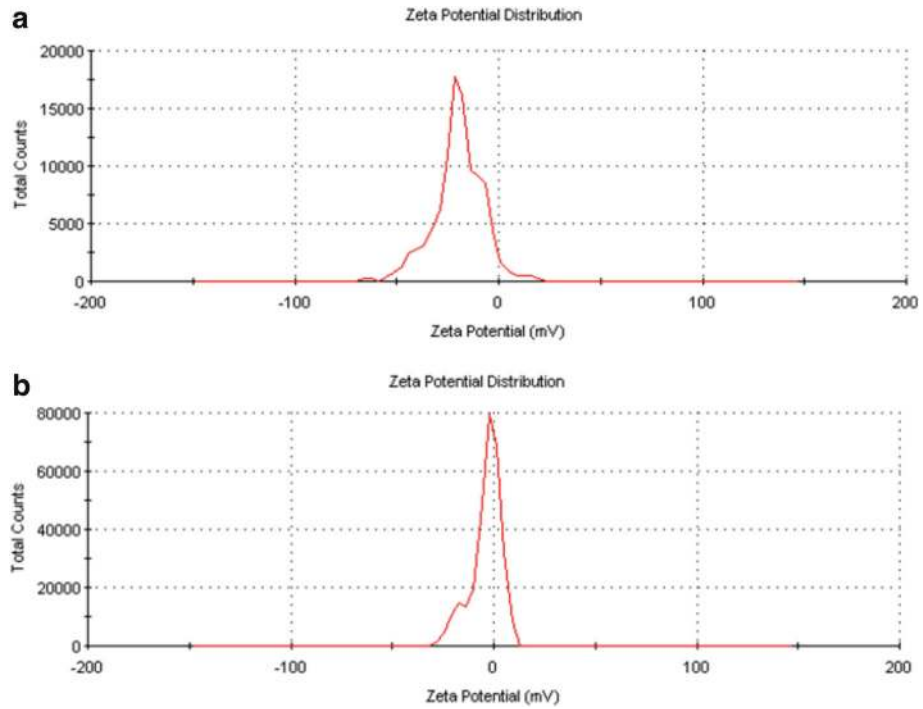

Fig. 9 Zeta potential of AgNPs synthesized by *Trichoderma longibrachiatum* fungal biomass of **a** 10 g and **b** 15 g after filtration

PdI value and − 0.8 mV zeta potential. FTIR was used to confirm the stability of AgNPs, where it revealed two distinct peaks at 1635.34 and 3269.31 cm^{-1}. Similar results were obtained as mentioned earlier (Fig. 8). The stability of nanoparticles in solution is very important with respect to antimicrobial activity as unstable AgNPs will not be able to disperse homogeneously, thus reducing the efficacy.

Antifungal activity of biosynthesized AgNPs

Determination of the antifungal activity of AgNPs synthesized by *T. longibrachiatum* was performed against nine fungal isolates: *A. alternata*, *F. verticillioides*, *F. moniliforme*, *A. flavus*, *A. heteromorphus*, *P. glabrum*, *P. brevicompactum*, *P. grisea*, and *H. oryzae*. The inhibition effect of AgNPs was analyzed in PDA by using colony formation units showed in Table 1 and Fig. 10. In most studied fungi, high inhibition percentages of fungal colony formation were observed by comparing to the positive control of 1 mM $AgNO_3$ or the negative control (water). In the present results, AgNPs were most effective against *P. grisea*, *F. verticillioides*, *H. oryzae*, *F. moniliforme*, and *A. alternate* with inhibition percentages of 98.9, 96.4, 95.1, 93.6, and 93.0%, respectively. On other hand, the least efficiency of AgNPs was observed against *F. oxysporum* where it had 68.2% inhibition of colony formation. Statistical analysis showed that there were significant reductions ($P < 0.05$) in colony formation of the indicated fungal species resulting from the use of AgNPs and $AgNO_3$ compared to the control (Table 1). Several studies revealed that biosynthesized AgNPs can be applied effectively in the control of microorganisms and the prevention of deleterious infections. The inhibitory effect of AgNPs on plant pathogenic fungus *P. grisea* was reported by Young et al. (2009) and Elamawi and El-shafey (2013). Biosynthesized AgNPs from *T. longibrachiatum* improved seed germination percentage and vigor index and reduced the disease incidence caused by *F. oxysporium*, a seed-borne pathogen on faba bean, tomato, and barley (Elamawi and Al-Harbi 2014). The AgNPs of smaller dimensions in this study were shown to be the most efficient against the tested phytopathogenic fungi. In fact, several studies have shown that AgNP activity is strongly dependent on the nanoparticle size (Rahimi et al. 2016).

Durán et al. (2005) attributed the antimicrobial activity of AgNPs to the formation of insoluble compounds by inactivation of sulfhydryl groups in the fungal cell wall and disruption of membrane-bound enzymes and lipids resulting in lysis of cell. It was also reported that the process may involve the binding of AgNPs to external proteins to create pores, interfering with DNA replication or forming reactive oxygen species (ROS) such as hydrogen peroxide, superoxide anions, and hydroxyl radicals (Jung et al. 2008; Duran et al. 2016; Ottoni et al. 2017).

Conclusions

In conclusions *T. longibrachaitum* was used in the biosynthesis of silver nanoparticles. Such type of synthesis may be considered as eco-friendly as it is free from any toxic chemicals or organic solvents during the biosynthesis process. Optimization of various parameters was carried out, using a "one at a time" strategy keeping all other variables constant and varying only one. Incubation at 28 °C, fungal biomass at 10 g, without agitation, and incubation for 72 h resulted in biosynthesis of AgNPs by *T. longibrachaitum*. Dilution at 20% and filtration, using Millipore filter paper 0.22 μm, were favorable for measuring the particle size distribution, using DLS system. *T. longibrachiatum* showed a potential for extracellular and stable biosynthesis of silver nanoparticles, as confirmed by UV–vis spectroscopy, which showed an absorption peak at 385 nm. TEM revealed the formation of spherical nanoparticles with size ranging

Table 1 Inhibitory effect of synthesized AgNPs by *Trichoderma longibrachiatum* for different fungi

Fungal isolates	Colony formation/cm^2					
	Control	$AgNO_3$	$AgNO_3$ efficiency (%)	AgNPs	AgNP efficiency (%)	*P* value < 0.05
A. alternata	12.63	2.13	83.1	0.88	93.0	0.089
F. verticillioides	29.67c	6.67b	77.5	1.08a	96.4	0.002
F. moniliform	17.63c	2.44b	91.8	1.13a	93.6	0.00
A. flavus	25.63c	9.75b	62.0	3.42a	86.7	0.00
A. heteromorphus	10.17c	4.58b	55.0	1.67a	83.6	0.002
P. glabrum	28.08c	20.92b	25.5	6.83a	75.7	0.009
P. brevicompactum	24.67c	13.50b	45.3	1.75a	92.9	0.003
H. oryzae	5.33c	1.98b	62.9	0.26a	95.1	0.00
P. grisea	11.50c	2.13b	81.5	0.13a	98.9	0.001

Means followed by the same latter are not significantly different at the 0.05% level

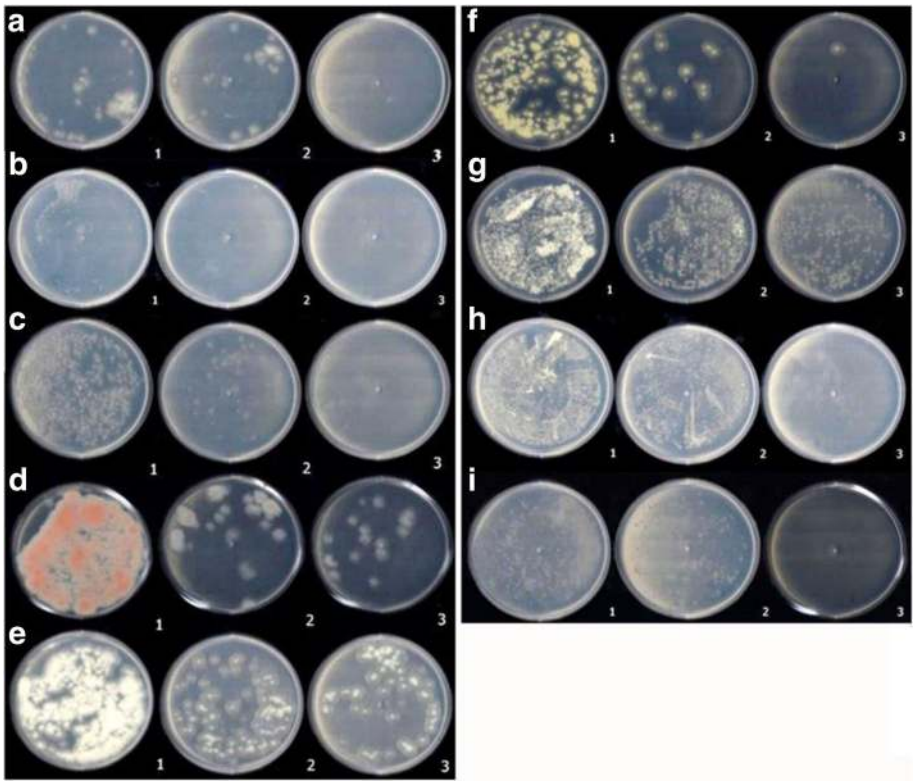

Fig. 10 Antifungal activity of different treatments, (1) control, (2) $AgNO_3$, and (3) silver NPs, for different microorganisms: **a** *Alternaria alternata*, **b** *Pyricularia grisea*, **c** *Fusarium verticillioides*, **d** *F. moniliform*, **e** *Aspergillus flavus*, **f** *A. heteromorphus*, **g** *Penicillium glabrum*, **h** *P. brevicompactum*, and **i** *Helminthosporium oryzae*

between 5 and 25 nm. FTIR showed the bands at 1634.92 and 3269.31 cm^{-1}. DLS supported that the *Z*-average (r.nm) was 24.43 nm and 0.420 PdI value. The zeta potential was – 19.7 mV with a single peak.

Further studies are still needed to understand the precise molecular mechanism leading to the formation of AgNPs by biological methods in order to have a better control over the size and polydispersity of these nanoparticles. Further research should focus on the development of silver compounds and mixing with fungicides. At the same time, the environmental tracking of silver when applied in the field is important to assess its impact on environment and human health. This information is imperative for future registration and labeling of the AgNPs if they are to be used as fungicides for crop protection.

Acknowledgements
This research project was supported by a grant from the "Research Center for Female Scientific and Medical Colleges," Deanship of Scientific Research, King Saud University.

Authors' contributions
All authors read and approved the final manuscript.

Competing interests
The authors declare that they have no competing interests.

Publisher's Note

Author details
[1]Rice Pathology Department, Plant Pathology Research Institute, Agricultural Research Center, PO Box 33717, Sakha, Kafr Elshiekh, Egypt. [2]College of Science, King Saud University, PO Box 22452, Riyadh, Saudi Arabia. [3]Physics Department, College of Science, King Saud University, PO Box 22452, Riyadh, Saudi Arabia.

Received: 27 September 2017 Accepted: 8 January 2018
Published online: 08 March 2018

References

Ahmad A, Mukherjee P, Senapati S, Mandal D, Khan MI, Kumar R, Sastry M (2003) Extracellular biosynthesis of silver nanoparticles using the fungus *Fusarium oxysporum*. Colloids Surf B Biointerfaces 28:313–318
AshaRani PV, Mun GLK, Hande MP, Valiyaveettil S (2009) Cytotoxicity and genotoxicity of silver nanoparticles in human cells. ACS Nano 3(2):279–290
Balaji DS, Basavaraja S, Deshpande R, Mahesh DB, Prabhakar BK, Venkataraman A (2009) Extracellular biosynthesis of functionalized silver nanoparticles by strains of *Cladosporium cladosporioides* fungus. Colloids Surf B Biointerfaces 68(1):88–92
Barnett, H.L. and Hunter, B.B. 1995. Illustrated genera of imperfect fungi fourth edition
Capek I (2004) Preparation of metal nanoparticles in water-in-oil (w/o) microemulsions. Adv Colloid Interf Sci 110(1-2):49–74

Das SK, Marsili E (2010) A green chemical approach for the synthesis of gold nanoparticles: characterization and mechanistic aspect. Rev Environ Sci Biotechnol 9:199–204
Durán N, Marcato PD, Alves OL, Souza G, Esposito E (2005) Mechanistic aspects of biosynthesis of silver nanoparticles by several *Fusarium oxysporum* strains. J Nanobiotechnol 3:1–8
Duran N, Nakazato G, Seabra AB (2016) Antimicrobial activity of biogenic silver nanoparticles, and silver chloride nanoparticles: an overview and comments. Appl Microbiol Biotechnol 100(15):6555–6570
Elamawi RM, Al-Harbi RE (2014) Effect of biosynthesized silver nanoparticles on *Fusarium oxysporum* fungus the cause of seed rot disease of faba bean, tomato and barley. J Plant Prot Path Mansoura Univ 1(12):991–1007
Elamawi RM, El-Shafey RA (2013) Inhibition effects of silver nanoparticles against rice blast disease caused by *Magnapor thegrisea*. Egypt J Agric Res 91(4):1271–1281
Emeka EE, Ojiefoh OC, Aleruchi C (2014) Evaluation of antibacterial activities of silver nanoparticles green-synthesized using pineapple leaf (Ananas comosus). Micron 57:1–5
Fayaz M, Balaji K, Girilal M, Yadav R, Kalaichelvan PT, Venketesan R (2010) Biogenic synthesis of silver nanoparticles and their synergistic effect with antibiotics: a study against grampositive and gram-negative bacteria. Nanomedicine 6:103–109
Fayaz M, Balaji K, Kalaichelvan PT, Venkatesan R (2009) Fungal based synthesis of silver nanoparticles—an effect of temperature on the size of particles. Colloids Surf. B. Biointerfaces 74:123–126
Gole AC, Dash V, Ramakrishnan SR, Sainkar AB, Mandale M, Sastry M (2001) Pepsin gold colloid conjugates, preparation, characterization, and enzymatic activity. Langmuir 17:1674
Harman AE (2006) Overview of mechanisms and uses of *Trichoderma* spp. Phytopathology 96(2):190–194
Harman GE, Howell CR, Viterbo A, Chet I, Lorito M (2004) Trichoderma species—opportunistic avirulent plant symbionts. Nat Rev Microbiol 2(1):43–56
Huang J, Zhan G, Zheng B, Sun D, Lu F, Lin Y, Chen H, Zheng Z, Zheng Y, Li Q (2011) Biogenic silver nanoparticles by *Cacumen Platycladi* extract: synthesis, formation mechanism and antibacterial activity. Ind Eng Chem Res 50:9095–9106
Ingle A, Gade A, Pierrat S, Sonnichsen C, Rai M (2008) Mycosynthesis of silver nanoparticles using the fungus *Fusarium acuminatum* and its activity against some human pathogenic bacteria. Curr Nanosci 4(2):141–144
Jaidev LR, Narasimha G (2010) Fungal mediated biosynthesis of silver nanoparticles, characterization and antimicrobial activity. Colloids Surf B 81:430–433
Jain N, Bhargava A, Majumdar S, Tarafdar JC, Panwar J (2011) Extracellular biosynthesis and characterization of silver nanoparticles using *Aspergillus flavus* NJP08: a mechanism perspective. Nano 3:635–641
Jeong SH, Yeo SY, Yi SC (2005) The effect of filler particle size on the antibacterial properties of compounded polymer/silver fibers. J Mater Sci 40(20):5407–5411
Jung WK, Koo HC, Kim KW, Shin S, Kim SH, Park YH (2008) Antibacterial activity and mechanism of action of the silver ion in *Staphylococcus aureus*and *Escherichia coli*. Appl Environ Microbiol 74(7):2171–2178
Kim YS, Kim JS, Cho HS, Rha DS, Kim JM, Park JD, Choi BS, Lim R, Chang HK, Chung YH, Kwon IH, Jeong J, Han BS, Yu IJ (2008) Twenty-eight day oral toxicity, genotoxicity, and gender-related issue distribution of silver nanoparticles in Sprague-Dawley rats. Inhal Toxicol 20:575–583
Kotakadi VS, Gaddam SA, Venkata SK, Sarma PVGK, Sai Gopal DVR (2016) Biofabrication and spectral characterization of silver nanoparticles and their cytotoxic studies on human CD34 +ve stem cells. Biotech 6(2):216
Mandal S, Phadtare S, Sastry M (2005) Interfacing biology with nanoparticles. Curr Appl Phys 5(2):118–127
Mukherjee P, Senapati S, Mandal D (2002) Extracellular synthesis of gold nanoparticles by the fungus *Fusarium oxysporum*. Chem Bio Chem 3(5):461–463
Murphy M, Ting K, Zhang X, Soo C, Zheng Z (2015) Current development of silver nanoparticle preparation, investigation, and application in the field of medicine. J Nanomater 2015:1–12
Nair AS, Pradeep T (2003) Halocarbon mineralization and catalytic destruction by metal nanoparticles. Curr Sci 84:1560–1564
Ottoni CA, Simaes MF, Fernandes S, Santos JG, da Silva ES, Souza RFB, Maiorano AE (2017) Screening of filamentous fungi for antimicrobial silver nanoparticles synthesis. AMB Expr 7:31–41
Pal S, Tak YK, Song JM (2007) Does the antibacterial activity of silver nanoparticles depend on the shape of the nanoparticle ? A study of the gram-negative bacterium *Escherichia coli*. Appl Environ Microbiol 73(6): 1712–1720
Rahimi G, Alizadeh F, Khodavandi A (2016) Mycosynthesis of silver nanoparticles from Candida albicans and its antibacterial activity against *Escherichia coli* and *Staphylococcus aureus*. Trop J Pharm Res 15(2):371–375
Rai M, Yadav A, Gade A (2009) Silver nanoparticles as a new generation of antimicrobials. Biotechnol Adv 27(1):76–83
Roy S, Mukherjee T, Chakraborty S, Kumar das T (2013) Biosynthesis, characterisation and antifungal activity of silver nanoparticles by the fungus *Aspergillus foetidus* MTCC8876. Digest J NanomaterBiostruct 8:197–205
Sastry M, Ahmad A, Islam NI, Kumar R (2003) Biosynthesis of metal nanoparticles using fungi and actinomycete. Curr Sci 85:162–170
Schultz S, Smith DR, Mock JJ, Schultz DA (2000) Single-target molecule detection with nonbleaching multicolor optical immunolabels. PNAS 97:996–1001
Sharma VK, Yngard RA, Lin Y (2009) Silver nanoparticles: green synthesis and their antimicrobial activities. Adv Colloid Interf Sci 145(1-2):83–96
Singh P, Balaji RB (2011) Biological synthesis and characterization of silver nanoparticles using the fungus *Trichoderma harzianum*. Asian J Exp Biol Sci 2:600–605
Sivasithamparam K, Ghisalberti EL (1998) Secondary metabolism in *Trichoderma* and *Gliocladium*. In: Kubicek CP, Harman GE (eds) *Trichoderma* and *Gliocladium* (1) basic biology, taxonomy and genetics. Taylor and Francis Ltd., London, pp 139–191
Solanki JN, Murthy ZVP (2010) Highly monodisperse and sub-nano silver particles synthesis via microemulsion technique. Colloids Surf A Physicochem Eng Asp 359:31–38
Solomon SD, Bahadory M, Jeyarajasingam AV, Rutkowsky SA, Boritz C (2007) Synthesis and study of silver nanoparticles. J Chem Educ 84:322–325
Sondi I, Salopek-Sondi B (2004) Silver nanoparticles as antimicrobial agent, a case study on *E. coli* as a model for Gram-negative bacteria. J Colloid Interface Sci 275:177–182
Suresh AK, Doktycz MJ, Wang W, Moon JW, Gu B, Meyer HM III, Hensley DK, Allison DP, Phelps TJ, Pelletier DA (2011) Monodispersed biocompatible silver sulfide nanoparticles: facile extracellular biosynthesis using the γ-proteobacterium *Shewanella oneidensis*. Acta Biomater 7:4253–4258
Vahabi K, Mansoori GA, Karimi S (2011) Biosynthesis of silver nanoparticles by fungus *Trichoderma reesei* (a route for large-scale production of AgNPs). Insciences J 1(1):65–79
Vandebriel RJ, Tonk ECM, de la Fonteyne-Blankestijn LJ, Gremmer ER, Verharen HW, van der Ven LT, van Loveren H, de Jong WH (2014) Immunotoxicity of silver nanoparticles in an intravenous 28-day repeated-dose toxicity study in rats. Part Fibre Toxicol 11(21):1–9
Wang Z, Chen J, Yang P, Yang W (2007) Biomimetic synthesis of gold nanoparticles and their aggregates using a polypeptide sequence. ApplOrganomet Chem 21(8):645–651
Young KJ, Byung HK, Geunhwa J (2009) Antifungal activity of silver ions and nanoparticles on phytopathogenic fungi. Plant Dis 93:1037–1043